Mater. Res. Soc. Symp. Proc. Vol. 1744 © 2015 Materials Research Society
DOI: 10.1557/opl.2015.503

Glass Corrosion in the Presence of Iron-Bearing Materials and Potential Corrosion Suppressors

Joelle Reiser[1], Lindsey Neill[1], Jamie Weaver[1], Benjamin Parruzot[1], Christopher Musa[1], James Neeway[2], Joseph Ryan[2], Nikolla Qafoku[2], Stéphane Gin[3], Nathalie A. Wall[1]

[1] Washington State University, Chemistry Department, Pullman, WA 99164, USA
[2] Pacific Northwest National Laboratory, Energy and Environment Directorate, Richland, WA 99352, USA
[3] CEA Marcoule DTCD/SECM, F-30207 Bagnols-sur-Cèze, France

ABSTRACT

A complete understanding of radioactive waste glass interactions with near-field materials is essential for appropriate nuclear waste repository performance assessment. In many geologic repository designs, Fe is present both in the natural environment and in the containers that will hold the waste glasses. In this paper we discuss investigations of the alteration of International Simple Glass (ISG) in the presence of Fe^0 foil and hematite (Fe_2O_3). Based on solid analysis, ISG alteration is more pronounced in the presence of Fe^0 than with hematite. Additionally, typical glass corrosion is observed for distances of 5 mm between Fe materials and ISG, but incorporation of Fe in the alteration layer is only observed for systems exhibiting full contact between Fe^0 material and ISG. Solution analysis results indicate that diatomaceous earth minimizes corrosion to a larger extent than fumed silica does when present with iron and ISG.

INTRODUCTION

The understanding of the long-term evolution of borosilicate glasses is of particular importance for the disposal of high-level radioactive waste (HLW) [1, 2, 4], and glass alteration in the presence of near-field materials must be known [2, 3]. Iron is a particularly important near-field material since it is in the natural environment and in the stainless steel containers that store the waste glass [2]. Iron also is a component that is present in many waste glasses. When in the 2+ oxidation state in solution, iron is known to accelerate the glass alteration rate but the corresponding mechanisms are not fully understood [3]. This work presents experimental results regarding 1) glass alteration in the presence of Fe^0 and Fe_2O_3 to evaluate the effect of the Fe oxidation state on glass alteration and 2) the efficacy of potential glass corrosion suppressants at 90°C: diatomaceous earth (DE) and fumed silica (FS). International Simple Glass (ISG) was used for these studies; ISG, a six-component borosilicate glass, was developed as a reference benchmark glass for an international collaboration on waste glass alteration mechanisms [4].

EXPERIMENT

Materials

International Simple Glass (ISG) has a density of 2.5 $g \cdot cm^{-3}$ and a composition in weight percentages as follows: SiO_2: 56.2%, B_2O_3: 17.3%, Na_2O: 12.2%, Al_2O_3: 6.1%, CaO: 5.0% and ZrO_2: 3.3% [5]. The glass was obtained in bar form from Savannah River National Laboratory. Coupons were cut with a low-speed saw with a diamond tipped blade (Buehler Isomet®). The

coupons were polished on a Leco Grinding and Polishing® SS-200 polisher up to 1200 grit. Dimensions of each coupon were approximately 10 × 20 × 2 mm^3. Hematite coupons (Fisher®) were cut to the same dimensions as the glass coupons and polished to 320 to 600 grit. Fe^0 foil (Sigma Aldrich®) of thickness 0.1 mm was cut to two of the same dimensions as the coupons 10 × 20 mm^2. Diatomaceous earth (DE) (MP-Biomedicals®) and fumed silica (SiO_2, called FS hereafter) (Sigma Aldrich®) were prepared as powders; DE was sieved to 149 – 250 µm, and FS was available at 0.2 – 0.3 µm. Deionized distilled water (18 MΩ) (DIW) was used.

Assembly Description

Figure 1 presents the experimental setups. The configuration in Figure 1a allows for determination of ISG corrosion in the presence of iron sources and as a function of the distance between the iron source and glass (both 0 mm – i.e. full contact – and 5 mm). Previous studies showed the importance of a complete contact between the iron source and the glass coupons, which allows for uniform glass corrosion [3]. In the present work, Fe^0 foil was etched with a knife in a grid pattern to facilitate solution flow between ISG and the Fe^0 foil. The etched Fe^0 foil was flattened with a metal roller onto the ISG coupon, and the polished hematite coupon was pressed against the ISG surface. The gap between the two ISG coupons was maintained by 5 mm Teflon® spacers, and the sample configurations were held together with chemically inert glue (Loctite® Plastics Bonding System). Solution was allowed to flow along every surface of the glass except the portions touching the Teflon® blocks. Additional Teflon® spacers were used to elevate the bottom ISG coupon from the experimental stainless steel vessel (50 mL Parr®). The efficacy of glass corrosion suppressant (CS) – DE or FS – in the presence of Fe^0 was tested using the set-up presented in Figure 1b. The CS was placed in a bag made of 30 micron nylon mesh (Industrial Netting®) between the Fe^0 foil and the top ISG coupon, while the bottom ISG coupon remained out of contact with the CS. Solution was allowed to flow through the mesh bag to allow for every glass surface to be in contact with solution with the exception of portions in contact with the Teflon® blocks. Additionally, blank samples were prepared: Teflon® blocks and glue; ISG with Teflon® blocks and glue; FS with Teflon® blocks and glue, DE with Teflon® blocks and glue; ISG with DE, Teflon® blocks, and glue; and ISG with FS, Teflon® blocks, and glue. The following nomenclature is used to designate experimental setups: ISG/iron source/CS (e.g. ISG/Fe/DE means ISG alteration in the presence of Fe^0 and DE, ø indicates the absence of iron source or CS). Each sample set was prepared in duplicates for statistical analysis.

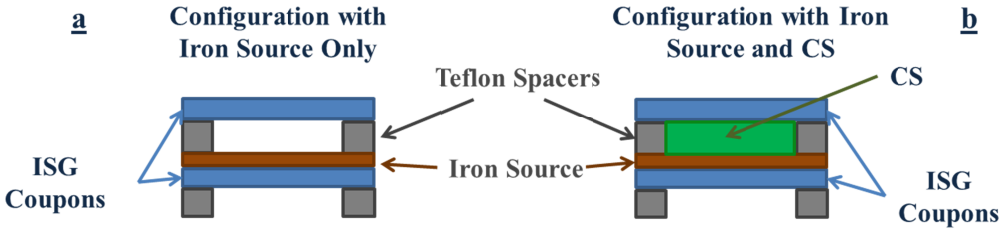

Figure 1: Schematic Representation of the Experimental Configurations with a) Iron Source Only and b) Iron Source and Corrosion Suppressant (CS)

Each configuration was inserted into Parr® vessels containing 25 mL DIW to obtain a glass-surface-area-to-solution-volume ratio (S/V) of 40 m^{-1} with the exception of ISG/ø/ø which had an S/V of 20 m^{-1}. The solutions were purged with pure N_2 (A-L Compressed Gases, Inc.) and

solution pH was measured at room temperature before sealing the Parr® vessels. All experiments were carried out in a 90°C oven for 1 month without disturbing the samples. Losses due to evaporation were negligible. The solutions were then removed and pH was measured at room temperature. Glass samples were washed with ethanol and dried in a desiccator. ISG samples were then cut for various analyses.

Characterization Techniques

Solutions were diluted with 1-2% HNO_3 and analyzed using Inductively Coupled Plasma Optical Emission Spectrometry (ICP-OES) (Perkin Elmer® Optima 3200 RL) for Al, B, Ca, Fe, Na, and Si; the instrument was calibrated using dilutions of standard solutions (Inorganic Ventures).

Normalized loss (NL_x) of B, Si, and Na from ISG in $g \cdot m^{-2}$ was calculated using the following equation:

$$NL_x = \frac{C_X}{\left(\frac{S}{V}\right) f_X} \quad (1)$$

Where C_X is the elemental concentration in $g \cdot m^{-3}$, f_X is the mass fraction of the selected element in ISG, and S/V in m^{-1}. NL(Si) is corrected for excess Si for samples that contained fumed silica, based on Si concentration determined in ø/ø/FS configurations. This correction is calculated from the Si release of a sample of fumed silica altered in water for one month. This correction could not be applied to the samples containing DE due to experimental error associated with the Si concentration for the ø//ø/DE blank.

Altered monoliths were embedded in epoxy resin (Specifix-20®) polished to 1200 grit and sectioned to expose the cross section. Altered and unaltered glass compositions were measured by Energy-Dispersive X-ray Spectrometry (EDS) using the JEOL JXA-8500F electron microprobe, equipped with a Thermo Scientific UltraDry EDS detector and ThermoNORAN™ System 7 analytical software. Measurements were made using an accelerating voltage of 15 kV, and a beam current of 8 nA. The beam was defocused to a 1µm spot size to help mitigate alkali migration under beam irradiation [6]. Due to the roughness of the surfaces, quantitative data could not yet be obtained from EDS analyses. The thickness of the alteration layer was measured using the SEM images of the cross sections and ImageJ software. Alteration layer thickness was measured at multiple points on a glass side to allow for statistical analysis.

DISCUSSION

Over the course of the experiment, sample solution pH increased from a range of 5.0 - 6.0 to 7.5 - 9.5. Figure 2 shows NL_x for B, Na, and Si. Uncertainty is reported as twice the standard deviation associated with results obtained from duplicate analyses. Boron is used as a tracer of glass alteration because B is known to not be retained in the alteration products. NL(B) and NL(Na) are comparable for most samples for the chosen S/V of 40 m^{-1}. NL(Si) is smaller than NL(B) and NL(Na) for each sample; NL(Si) is particularly small for ISG/Fe/ø. In general, samples featuring corrosion suppressants, FS or DE, have lower NL(B) than their counterparts in absence of FS or DE, indicating that corrosion suppression is occuring. However, there is no statistical difference between NL(B) values for ISG/Fe/ø and ISG/Fe/FS. At this point, FS is not

known to be an appropiate suppressant for ISG corrosion in the presence of Fe^0. NL(B) is slightly smaller for ISG/Fe/DE than for ISG/Fe/FS.

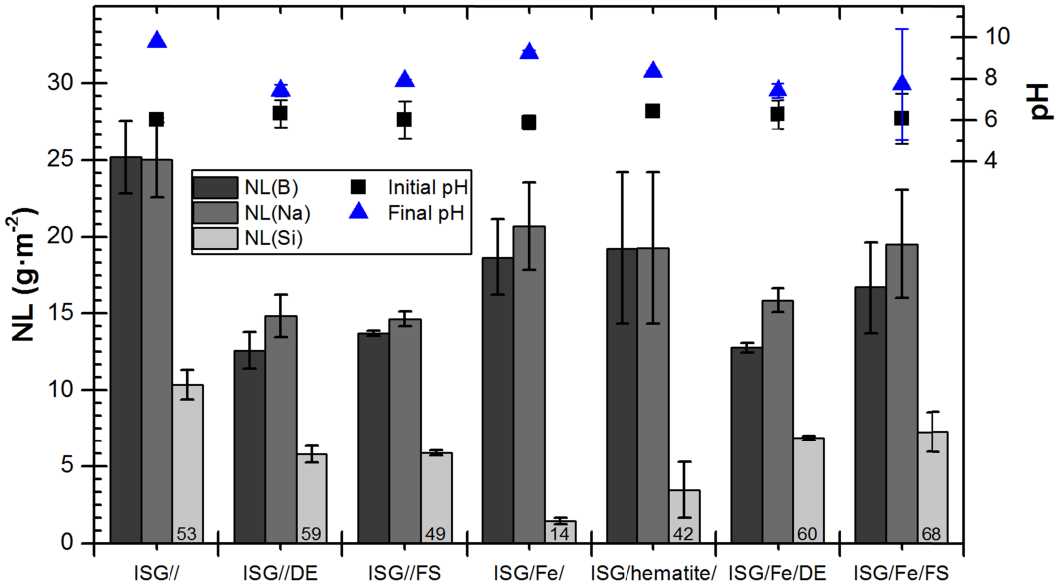

Figure 2: Normalized mass losses (NL_x) for each sample calculated from solution concentrations of B, Na, and Si (left axis), initial and final solution pH (right axis), and corrected concentrations of Si in ppm shown in the NL(Si) bars

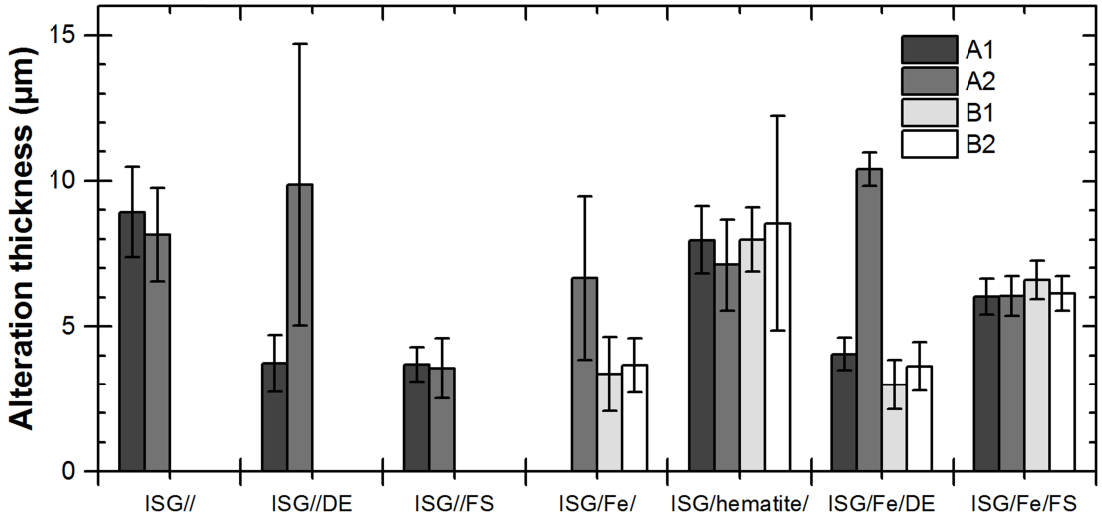

Figure 3: Alteration thickness measurements obtained from SEM cross sections of altered coupons. The labels indicate the identity of the glass coupon and its side and refer to the drawing, with A1 being the top side of the upper glass coupon, for example. SEM micrographs will be provided in another manuscript.

The alteration layer thicknesses of the various surfaces are shown in Figure 3; alteration layers were not observed on all surfaces because the layers were too thin. Additionally, the surface in contact with iron (B1) in ISG/Fe/DE, ISG/Fe/FS, and ISG/Fe/ø configurations had

alteration layers that contained iron as indicated by EDS spectra. A2 alteration layers did not contain iron, but secondary products featuring trace levels of iron were observed at the surface of the altered glass coupon. Within a single sample, alteration layer thicknesses are not identical within reported uncertainty for ISG/ø/DE (A1 and A2) and ISG/Fe/DE (A2 versus all the other coupon sides). For all the other samples, alteration thicknesses do not vary between glass coupon sides. However, for the surface of the top coupon in contact with the mesh bag that contains the CS, the alteration thickness is larger for ISG/Fe/FS than for ISG/Fe/DE for surfaces B1 and B2, and the alteration thickness is larger for ISG/hematite/ø than for ISG/Fe/ø. Comparison between ISG/ø/ø and ISG/Fe/ø shows no statistical difference between their results at A2, indicating that the upper coupon is too far from the Fe source for Fe to influence alteration. .

NL_x values determined from solution analysis can be converted to an equivalent altered glass thickness based on the density of ISG. This equivalent altered glass thickness is an average value over the whole glass surface area, S, and can thus be compared to the average of the 4 alteration layer thicknesses obtained from solid state analysis measurements (A1, A2, B1 and B2). Figure 4 shows the comparison of alteration layer thickness from solution and solid state analysis. The dashed columns on Figure 4 represent configurations that featured Fe in the some alteration layers. For configurations ISG/ø/ø, ISG/ø/DE, ISG/Fe/DE, and ISG/Fe/FS, the calculated solution and measured solid alteration thicknesses are statistically equivalent.

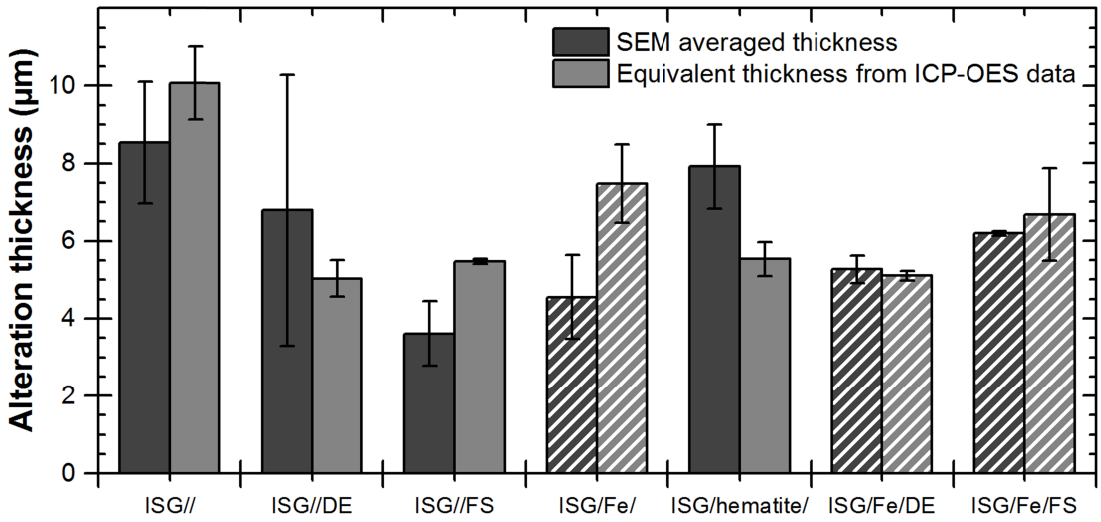

Figure 4: Alteration Thickness Comparison. Dashed columns: presence of Fe in some alteration layers.

The alteration thickness for ISG/Fe/ø measured by SEM is statistically smaller than the thickness determined from solution data; this may be due to calculation artifacts that do not account for the fact that the presence of Fe in the alteration layer increases the layer density. The differences between the resulting alteration thicknesses for ISG/hematite/ø can be due to an excessive amount of glue on the surface of the coupons that reduced the glass surface area in contact with water. The apparent differences observed for the ISG/ø/FS alteration thicknesses deducted from either solution or solid analysis will be investigated further with additional long-term experiments.

CONCLUSIONS

Results presented in this paper are preliminary data for further work, in which similar glass corrosion tests will be run for longer time periods and the distance between upper glass coupons and Fe sources will be decreased. Additionally, the phases into which Fe is incorporated in the alteration layer will be investigated.

ACKNOWLEDGMENTS

This research is being performed using funding received from the DOE Office of Nuclear Energy's Nuclear Energy University Programs, under Project 23-3361.The authors would like to thank Dr. Owen Neill of the WSU School of the Environment for his assistance with the electron microprobe solid state analysis.

REFERENCES

[1] E. Burger, D. Rebiscoul, F. Bruguier, M. Jublot, J. E. Lartigue, and S. Gin, "Impact of iron on nuclear glass alteration in geological repository conditions: A multiscale approach," *Appl. Geochemistry*, vol. 31, pp. 159–170, Apr. 2013.

[2] B. Fleury, N. Godon, A. Ayral, and S. Gin, "SON68 glass dissolution driven by magnesium silicate precipitation," *J. Nucl. Mater.*, vol. 442, no. 1–3, pp. 17–28, Nov. 2013.

[3] A. Michelin, E. Burger, E. Leroy, E. Foy, D. Neff, K. Benzerara, P. Dillmann, and S. Gin, "Effect of iron metal and siderite on the durability of simulated archeological glassy material," *Corros. Sci.*, vol. 76, pp. 403–414, Nov. 2013.

[4] S. Gin, a. Abdelouas, L. J. Criscenti, W. L. Ebert, K. Ferrand, T. Geisler, M. T. Harrison, Y. Inagaki, S. Mitsui, K. T. Mueller, J. C. Marra, C. G. Pantano, E. M. Pierce, J. V. Ryan, J. M. Schofield, C. I. Steefel, and J. D. Vienna, "An international initiative on long-term behavior of high-level nuclear waste glass," *Mater. Today*, vol. 16, no. 6, pp. 243–248, Jun. 2013.

[5] Y. Inagaki, T. Kikunaga, K. Idemitsu, and T. Arima, "Initial Dissolution Rate of the International Simple Glass as a Function of pH and Temperature Measured Using Microchannel Flow-Through Test Method," *Int. J. Appl. Glas. Sci.*, vol. 4, no. 4, pp. 317–327, Dec. 2013.

[6] C. H. Nielson and H. Sigurdsson, "Quantitative methods for electron microprobe analysis of sodium in natural and synthetic glasses," *Am. Mineral.*, vol. 66, pp. 547–552, 1981.